Molecular Motors

DOI: 10.1002/ange.201202674

B_{13}^+: A Photodriven Molecular Wankel Engine**

Jin Zhang, Alina P. Sergeeva, Manuel Sparta, and Anastassia N. Alexandrova**

Synthetic molecular motors that are capable of delivering controlled movement upon energy input are one of the key building blocks in nanomachinery.[1] The major energy sources of molecular motors are from chemical reactions,[1a] photon beams,[1b] or electric current,[1f] which are converted into mechanical forces through the excitation of the electronic states of the molecule. The energy scale of the electronic excitation is normally two orders of magnitude larger than the molecular vibrational frequencies. To reduce the heat dissipation and increase the energy utilization efficiency, a motor running purely on the electronic ground-state (GS) potential energy surfaces is highly desirable.

Nanoclusters, which are neither molecules nor fragments of solids, are unique chemical species with remarkable novel structures, chemical bonding, and unexpected reactivity.[2] Recently, two planar boron clusters, B_{19}^- and B_{13}^+, have been demonstrated to undergo a rare fluxional behavior: the outer ring rotates almost freely with respect to the inner ring.[3–5] These clusters are anomalously stable species of low reactivity,[3,6,7] similar to their prototypical organic aromatic congeners: benzene and coronene.[2b,c,3,5,8] The low energy barrier that made the in-plane rotation possible was due to the delocalized bonding, which rendered concentric double aromaticity of both equilibrium and transition states of the clusters.[4,5] This peculiar fluxionality of B_{19}^- and B_{13}^+ at room temperature has gained them the name of "molecular Wankel motors".[4,5]

In equilibrium, driven by thermal fluctuations, the outer-ring rotation is bidirectional, and has a timescale of the order of tens of picoseconds at 300 K. To utilize B_{13}^+ as an engine for nanomachinery, an energy source is needed to drive the molecule out of equilibrium. Herein, we show that a unidirectional rotation of the outer ring of B_{13}^+ can be achieved with a circularly-polarized infrared (IR) laser, rendering a photodriven molecular Wankel motor running on the electronic GS potential energy surfaces with a rotational period of a few picoseconds.

The ground-state (GS) geometry of B_{13}^+, which exhibits C_{2v} symmetry, is shown in Figure 1 a. In equilibrium, B_{13}^+ has a small intrinsic dipole moment (0.4 Debye) along the C_{2v} axis, through which we define the square ring as the head of the molecule. Without an electric field, a complete 360° rotation of the outer ring is decomposed into 30 identical elementary moves (see Figure 3 of Ref. [5] for a detailed description). Each elementary move induces a slight relative movement between the inner and the outer ring. In Figure 1 a, through the sequence 1→2→3→4, all atoms in the outer ring B_{10} are rotated counterclockwise by one atomic position. A 36° rotation is thus completed through three consecutive elementary moves. During each move, a reorientation of the molecule takes place and rotates the head counterclockwise by 120°. This discretized reorientation of the molecule is critical to the guided unidirectional rotation of the outer ring, as will be shown below.

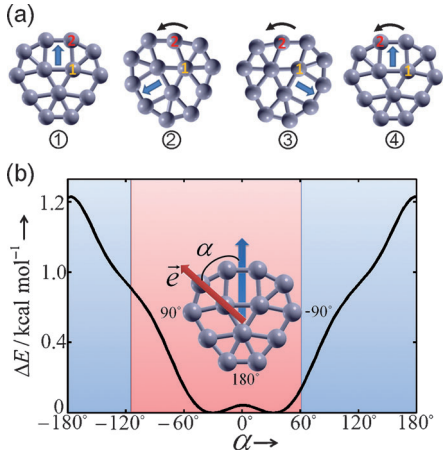

Figure 1. a) The outer-ring rotation. Three identical counterclockwise elementary rotations are involved in the sequence 1→2→3→4. The orientation of the molecule is defined by the upright arrow, which is aligned with the C_{2v} axis of the molecule. b) Relative ground-state energies of the elementary rotation of B_{13}^+ as a function of the angle α when a constant electric field ($|\vec{e}| = 2.6\times10^9\ V\,m^{-1}$) is applied. α (< 180°) is defined as the angle between the field direction and the molecule. The side (middle) region indicates that a counterclockwise rotation depicted in (a) is favored (unfavored) at a given angle α (see text for details).

When subjected to an electric field, the delocalized orbitals of the molecule are easily polarized. We found that the molecule has a tendency to line-up with the field to minimize the field component normal to the molecular plane. As an electric field can always be decomposed into in-plane and out-of-plane components, and a field perpendicular to the

[*] Dr. J. Zhang, Dr. M. Sparta, Prof. A. N. Alexandrova
Department of Chemistry and Biochemistry
University of California Los Angeles
607 Charles E. Young Drive East, Box 951569
Los Angeles, CA 90095-1569 (USA)
E-mail: jinzhang@chem.ucla.edu
ana@chem.ucla.edu
Homepage: http://www.chem.ucla.edu/~ana/
Dr. A. P. Sergeeva
Department of Chemistry and Biochemistry, Utah State University
Logan, UT 84322 (USA)

[**] Financial support for this work was provided through the ACS PRF grant 51052-DNI6 (A.N.A.). Alina P. Sergeeva is grateful to the NSF for the support through the CHE-1057746 grant.

Supporting information for this article is available on the WWW under http://dx.doi.org/10.1002/anie.201202674.

molecular plane does not affect any in-plane rotation, in the following we limit our discussion to the in-plane 2D case in which the electric field and the molecule are coplanar. We characterize the orientation of the molecule with respect to the field direction by the angle α (Figure 1b).

By studying the GS energies as a function of α, we found two energy minima which approximately correspond to $\alpha = \pm 30°$. Because the energy scale of the thermal fluctuation at room temperature is 0.6 kcal mol^{-1}, a fairly large portion of the bottom region with relatively small α is thermally reachable. For larger values of α, the configuration becomes gradually energetically unfavorable.

There are two ways to lower the total energy in the regions of large α: 1) rotating the molecule as a whole until α falls into the favorable region; 2) rotating the outer ring with an elementary rotation and change the orientation of the molecule by $\pm 120°$. Route 1 and route 2 do not only differ in energies but also in rotation characteristics. In route 1, the molecule rotates as a whole continuously, descending along the energy curve until reaching one of the minima in Figure 1b. In route 2, the outer ring rotates with respect to the inner triangle through elementary moves, each of which rotates the head of the molecule by a fixed amount, $\pm 120°$. There is no guarantee that the final state has a lower energy. For example, for any $\alpha_0 < 60°$, an elementary rotation towards either direction gives $|\alpha'_0| \equiv |\alpha_0 \pm 120°| > 60°$, which suggests that any re-orientation of the molecule through route 2 starting with α_0 always increases the total energy. Statistically, this region may be considered as a forbidden zone for an elementary rotation. The forbidden region for the counterclockwise move depicted in Figure 1a can be similarly deduced. In Figure 1b, the middle region is energetically allowed (shown in red) whereas the outer region is unfavored (shown in blue). In each elementary rotation, the work/heat produced can be estimated from the difference in the GS energies before and after the rotation, which reaches approximately 0.5 kcal mol^{-1}. The heat can be dissipated to a thermal bath at 300 K (0.6 kcal mol^{-1}) without causing significant increase in the molecular temperature.

When a constant electric field is applied, the symmetry of the potential energy surface is broken owing to the interaction with the moderately expressed dipole moment of B_{13}^+. This promotes a unidirectional rotation of the molecule. We also found that under an electric field the vibrational frequency of the elementary rotational mode varies drastically between 0 and 160 cm^{-1}. For $125° < \alpha < 160°$, the molecular geometry is no longer stable and deforms (rotates) spontaneously.

We consider the transition path of two elementary rotations towards opposite directions with an initial state of $\alpha = 90°$ (Figure 2). For other initial states with stable geometries and $|\alpha_0| > 60°$, similar conclusions were found. Without an electric field, the clockwise and counterclockwise rotations are equally possible, with a small barrier of 0.25 kcal mol^{-1} separating the initial and the final state. However, once a constant electric field is applied, the final states for clockwise and counterclockwise rotation differ in energy significantly. What is more interesting is the fact that the transition state barrier for the counterclockwise rotation almost completely disappears, whereas the barrier for clockwise rotation increases more than three-fold, to 0.81 kcal mol^{-1}. This transition path is ideal for rotating the outer ring unidirectionally.

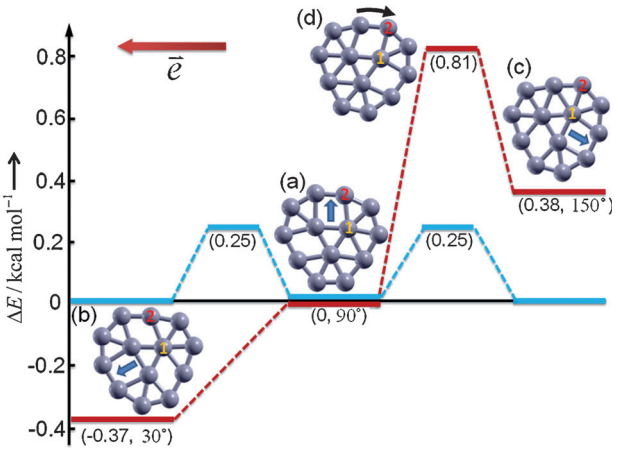

Figure 2. Energy profile of two elementary rotational moves (clockwise and counterclockwise) of the B_{13}^+ outer ring. a) The initial geometry; b,c) the final geometry after an elementary (counter)clockwise move; d) the transition state for the clockwise rotation. The blue line shows the transition path without electric field. When a constant electric field ($|\vec{e}| = 2.6 \times 10^9$ V m^{-1}) is applied, the counterclockwise rotation (a→b) is strongly favored over the clockwise rotation (a→c) with the transition path shown in the red line. There is almost no barrier for the counterclockwise move. The relative energies and angle α are given in parentheses. The marked B atoms and arrows are to guide the eye to illustrate the outer-ring rotation and changes in the orientation of the molecule.

The final step for a molecular Wankel motor design is to find a closed loop energy path along which the molecule is driven to work repeatedly. We propose that the molecule is driven with circularly polarized IR radiation along the path illustrated in Figure 3. The circularly-polarized electromagnetic wave is approximated as a (counter)clockwise rotating electric field at fixed frequency with constant modulus. In Figure 3a, the initial state is one of the states in the forbidden region, with some angle α_1 ($|\alpha_1| < 60°$). As the electric field rotating counterclockwise, α_1 gradually increases to some point α_2, at which the total energy is too high to maintain the geometry of the molecule stable. This phase P1 does not involve molecular reorientation (elementary rotation). Only the total energy of the molecule changes with the rotating field. The phase P2 is the reorientation process at α_2. Compared to the P1 phase, the time elapse of P2 is much shorter. Once the elementary rotation is finished, a new angle $\alpha' = \alpha - 120°$ is introduced. As long as $\alpha_2 < 180°$, the new angle is $|\alpha'| < 60°$. The system is restored to the P1 phase, and the loop is closed.

In Figure 3b, an example of the work loop proposed above is shown. The system starts from α_1 and is driven by a counterclockwise rotating field along the red line. At some point α_2, which is either randomly chosen by stochastic processes or is due to the unstable structure at large α_2, the outer ring undergoes a counterclockwise elementary rotation and re-orientates the molecule with a new angle $\alpha_1' = \alpha_2 - 120°$. The rotating field then keeps driving the system

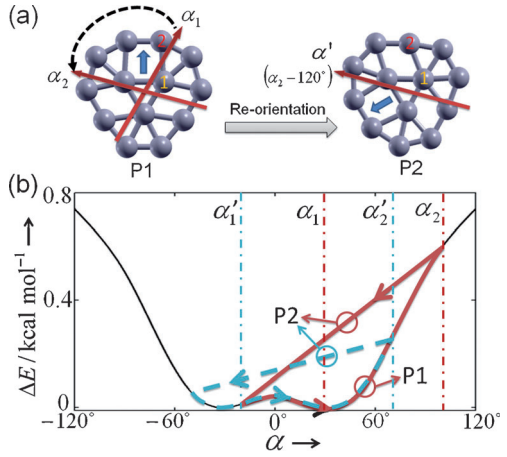

Figure 3. The elementary rotational move of the outer ring when guided by a circularly-polarized electric field. a) In phase P1, the field starts at $\alpha=\alpha_1$ ($|\alpha_1|<60°$) and rotates counterclockwise. There is no reorientation of the molecule occurring in P1. Once α reaches above 60°, the tendency of the molecule to undergo counterclockwise elementary rotation increases. At some point α_2 ($60°<\alpha_2<180°$), the molecule reorientates itself through an elementary rotation to lower its total energy. The new phase P2 has an angle $\alpha'=\alpha_2-120°$ owing to the reorientation, which brings $|\alpha'|<60°$. The cycle is completed and the system is back to P1 phase. b) Two example work loops of the proposed Wankel motor: $\alpha_1\rightarrow\alpha_2\rightarrow\alpha'_1\rightarrow\alpha'_2$. Marked with vertical dash-dotted lines, the angles $\alpha_{1,2}$ ($\alpha'_{1,2}$) are the starting points of phase P1/P2 on the red solid line (blue dashed line). In both loops, the lower branches are in P1 phase while the upper branches are in P2.

along the dashed line. Again at point α_2', the outer ring performs another counterclockwise rotation. Over time, the outer ring continues to rotate counterclockwise relative to the inner ring through a series of elementary rotations induced by closed loops similar to the red and blue lines shown in Figure 3b.

From above discussion, one sees that the (counter)clockwise rotating field promotes a (counter)clockwise rotation of the B_{13}^+ outer ring with respect to the inner one. What happens if the initial state falls out of the proposed phase, for example, $-180°<\alpha_1<-60°$ in Figure 3? The first possibility is that the molecule performs an elementary rotation, as it may not be stable or its total energy is high. In either direction, it will fall into one of the proposed phases. If the reorientation does not happen, the molecule remains largely structurally unchanged. As the field rotates, α_1 keeps increasing until it reaches the P1 phase. In either case, the outer-ring rotation of the molecule is synchronized.

To verify the proposed working principle of the molecular Wankel motor, we performed a Born–Oppenheimer molecular dynamics (BOMD) of a single B_{13}^+ ring at 600 K. The rotating electric field is simulated by rotating the molecule rigidly under a constant electric field at 3.1 THz. The frequency of the IR light is chosen in accordance with the intrinsic rotational time scale of the molecule determined by the temperature. In principle, an elementary rotation requires the electric field to rotate by 120°. In other words, a 360° rotation of the outer ring needs at least 10 loops of electric field rotation. In practice, because of thermal fluctuations, the gear ratio of this gearbox effect is expected to be higher than 10:1. With above parameters, we found the ratio was about 13:1.[13] Finally, to avoid exciting other degrees of freedom, the applicable frequency range of the IR radiation for the Wankel motor should be restricted to be below 160 cm^{-1}. The electric field strength we used in the simulation can be achieved experimentally by ultraintense lasers.

To realize such a motor in gas phase, the rigid rotation associated with the molecule needs to be considered. In Figure 1, there are two ways to lower the total energy when an electric field is applied. One is the rigid rotation of the molecule, and the other is the outer-ring rotation enabling the Wankel engine feature. Which route is more likely to be taken? According to the equipartition of kinetic energies, at room temperature, both the rigid rotation and the outer-ring rotation mode are thermally excited. The intrinsic thermal movement of atoms in the molecule at 300 K leads to a natural rotational frequency of the order of 100 GHz. For a laser field with THz frequency, the rigid rotation of the molecule is too slow to catch up with the field. On the other hand, for the unidirectional outer-ring rotation, by the gearbox effect (gear ratio ca. 10:1), the angular frequency of the outer-ring rotation can match the THz light frequency at 300 K. This makes the outer-ring rotation better promoted compared to the rigid rotation mode, as shown by the BOMD simulation.

In summary, we propose a model molecular Wankel motor B_{13}^+ driven by circularly polarized IR radiation near 3 THz, as a potential building block for nanomachines. The rotating frequency of the outer ring of is approximately 250 GHz. The recent discovery by Fokwa and Hermus of an embedded B_6 ring in a $Ti_7Rh_4Ir_2B_8$ crystal[9] points out a potential way of creating other unidirectional rotating molecular motors, based on pure boron, and other types of clusters.

Methods

Calculations were performed at density functional theory level with the Perdew–Burke–Ernzerhof (PBE) functional,[10] plane-wave basis set, and ultrasoft pseudopotentials implemented in Quantum Espresso.[11] For each B atom, 2s and 2p states occupied by three electrons were treated as valence states. The cutoff energy for the plane-wave basis set is 28 Ry. To minimize the long-range interaction among the periodic images, the Martyna–Tuckerman method[12] was adopted with an intermolecular distance of 15 Å. The electric field was applied as a sawtooth external potential with field strength fixed at $|\vec{e}|=2.6\times10^9\ V\,m^{-1}$ in the molecular region. BOMD was used to study the rotation of the molecule at finite temperatures (300–600 K). The rigid-body translational and rotational degrees of freedom were frozen initially by setting the initial velocities in the BOMD simulations but were allowed after the simulation started. The initial velocities were chosen to maintain the Boltzmann energy distribution of atomic kinetic energies.

Received: April 6, 2012
Revised: June 3, 2012
Published online: July 9, 2012

Keywords: ab initio calculations · Born–Oppenheimer molecular dynamics · boron · molecular motors · nanomachines

[1] a) T. R. Kelly, H. De Silva, R. A. Silva, *Nature* **1999**, *401*, 150–152; b) N. Koumura, R. W. J. Zijlstra, R. A. van Delden, N. Harada, B. L. Feringa, *Nature* **1999**, *401*, 152–155; c) E. R. Kay, D. A. Leigh, F. Zerbetto, *Angew. Chem.* **2006**, *119*, 72–196; *Angew. Chem. Int. Ed.* **2006**, *46*, 72–191; d) S. P. Fletcher, F. Dumur, M. M. Pollard, B. L. Feringa, *Science* **2005**, *310*, 80–82; e) T. R. Kelly, X. Cai, F. Damkaci, S. B. Panicker, B. Tu, S. M. Bushell, I. Cornella, M. J. Piggott, R. Salives, M. Cavero, Y. Zhao, S. Jasmin, *J. Am. Chem. Soc.* **2007**, *129*, 376–386; f) H. L. Tierney, C. J. Murphy, A. D. Jewell, A. E. Baber, E. V. Iski, H. Y. Khodaverdian, A. F. McGuire, N. Klebanov, E. C. H. Sykes, *Nat. Nanotechnol.* **2011**, *6*, 625–629; g) G. Pérez-Hernández, A. Pelzer, L. González, T. Seideman, *New J. Phys.* **2010**, *12*, 075007.

[2] a) A. P. Sergeeva, A. I. Boldyrev, *Aromaticity and Metal clusters* (Ed.: P. K. Chattaraj), CRC, Taylor & Francis Group, Boca Raton, **2010**, pp. 55–68; b) A. N. Alexandrova, A. I. Boldyrev, H. J. Zhai, L. S. Wang, *Coord. Chem. Rev.* **2006**, *250*, 2811–2866; c) D. Yu. Zubarev, A. P. Sergeeva, A. I. Boldyrev, *Chemical Reactivity Theory, A Density Functional View* (Ed.: P. K. Chattaraj), CRC, Taylor & Francis Group, New York, **2009**, pp. 439–452; d) *Physics and Chemistry of Small Metal Clusters* (Eds.: P. Jena, S. N. Khanna, B. K. Rao), Plenum, New York, **1987**; e) S. Sugano, *Microcluster Physics*, Springer, Berlin, **1991**; f) *Clusters of Atoms and Molecules* (Ed.: H. Haberland), Springer, Berlin, **1994**; g) *Quantum Phenomena in Clusters and Nanostructures* (Eds.: S. N. Khanna, A. W. Castleman, Jr.), Springer, Berlin, **2003**; h) T. D. Märk, A. W. Castleman, Jr., *Adv. Atomic Mol. Phys.* **1985**, *20*, 65–172; i) A. W. Castleman, Jr., R. G. Keesee, *Chem. Rev.* **1986**, *86*, 589–618; j) A. Ricca, C. W. Bauschlicher, *Chem. Phys.* **1996**, *208*, 233–242; k) F. L. Gu, X. M. Yang, A. C. Tang, H. J. Jiao, P. v. R. Schleyer, *J. Comput. Chem.* **1998**, *19*, 203–214; l) J. E. Fowler, J. M. Ugalde, *J. Phys. Chem. A* **2000**, *104*, 397–403.

[3] W. Huang, A. P. Sergeeva, H. J. Zhai, B. B. Averkiev, L. S. Wang, A. I. Boldyrev, *Nat. Chem.* **2010**, *2*, 202–206.

[4] J. O. C. Jiménez-Halla, R. Islas, T. Heine, G. Merino, *Angew. Chem.* **2010**, *122*, 5803–5806; *Angew. Chem. Int. Ed.* **2010**, *49*, 5668–5671.

[5] G. Martínez-Guajardo, A. P. Sergeeva, A. I. Boldyrev, T. Heine, J. M. Ugalde, G. Merino, *Chem. Commun.* **2011**, *47*, 6242–6244.

[6] L. Hanley, J. L. Whitten, S. L. Anderson, *J. Phys. Chem.* **1988**, *92*, 5803–5812.

[7] S. A. Ruatta, L. Hanley, S. L. Anderson, *J. Chem. Phys.* **1989**, *91*, 226–239.

[8] a) J. Aihara, *J. Phys. Chem. A* **2001**, *105*, 5486–5489; b) D. Y. Zubarev, A. I. Boldyrev, *Phys. Chem. Chem. Phys.* **2008**, *10*, 5207–5217.

[9] B. P. T. Fokwa, M. Hermus, *Angew. Chem. Int. Ed.* **2012**, *51*, 1702–1705.

[10] J. P. Perdew, K. Burke, M. Ernzerhof, *Phys. Rev. Lett.* **1996**, *77*, 3865–3868.

[11] P. Giannozzi, S. Baroni, N. Bonini, M. Calandra, R. Car, C. Cavazzoni, D. Ceresoli, G. L. Chiarotti, M. Cococcioni, I. Dabo, A. Dal Corso, S. de Gironcoli, S. Fabris, G. Fratesi, R. Gebauer, U. Gerstmann, C. Gougoussis, K. Kokalj, M. Lazzeri, L. Martin-Samos, N. Marzari, F. Mauri, R. Mazzarello, S. Paolini, A. Pasquarello, L. Paulatto, C. Sbraccia, S. Scandolo, G. Sclauzero, A. P. Seitsonen, A. Smogunov, P. Umari, R. M. Wentzcovitch, *J. Phys. Condens. Matter* **2009**, *21*, 395502.

[12] G. J. Martyna, M. E. Tuckerman, *J. Chem. Phys.* **1999**, *110*, 2810–2821.

[13] A video of the guided rotation of the outer ring can be found at http://www.chem.ucla.edu/~ana/movie/B13_11Rounds_Alt.MPG, where a total of 11 electric field rotations were performed.

